

# Flow-Induced Migration of Osteoclasts and Regulations of Calcium Signaling Pathways

CHENGLIN LIU, SHUNA LI, BAOHUA JI, and BO HUO

Biomechanics and Biomaterials Laboratory, Department of Mechanics, School of Aerospace Engineering, Beijing Institute of Technology, No. 5 South Zhongguancun Street, Beijing 100081, People's Republic of China

(Received 18 September 2014; accepted 3 December 2014; published online 31 December 2014)

Associate Editor Daniel Fletcher oversaw the review of this article.

**Abstract**—Osteoclasts are large multinucleate cells originating from the fusion of monocytes that are differentiated from hematopoietic stem cells. Although activated osteoclasts preferentially move to the area of microcrack by chemotaxis, whether such mechanical cues as fluid shear stress (FSS) regulate the migration of osteoclasts remains unknown. This study focuses on the effect of FSS on the migration of RAW264.7 monocytes and differentiated osteoclasts, as well as the roles of calcium signaling pathways in cell migration behaviors. We study five calcium signaling pathways, namely, mechanosensitive cation-selective channels (MSCC), phospholipase C, endoplasmic reticulum (ER), adenosine triphosphate, and extracellular calcium. Results show that FSS induces the migration of RAW264.7 cells along flow direction, and the directionality, alignment along the flow direction, and speed of cells are significantly enhanced with the increase in FSS levels. Blocking the pathways of MSCC, ER, or extracellular calcium significantly reduces the migration of RAW264.7 cells along the flow direction. However, the inhibition of calcium signaling pathways does not affect the migration behaviors after inducing RAW264.7 cells for 4 or 8 days with the conditioned medium. Therefore, this study indicates that both undifferentiated monocytes and differentiated osteoclasts tend to migrate along flow direction, furthermore the FSS-induced directional migration of the monocytes is regulated by calcium signaling pathways, but that of differentiated osteoclasts is unaffected.

**Keywords**—Osteoclast, Migration, Fluid shear stress, Calcium signaling, Differentiation.

## INTRODUCTION

Bone metabolism is maintained by the collective effort of osteoclasts and osteoblasts.<sup>13</sup> Osteoclasts are uniquely capable of resorbing bone matrix, whereas

osteoblasts are responsible for bone formation. Mature osteoclasts are highly specialized multinucleated cells formed by the fusion of marrow-derived mononuclear phagocytes (i.e., osteoclast precursors) that originated from hematopoietic stem cells induced by some cytokines, such as the macrophage-colony stimulating factor (M-CSF) and the receptor activator of NF- $\kappa$ B ligand (RANKL).<sup>2,31</sup> Bone resorption starts with the recruitment of mononucleated osteoclast precursors from circulation and proceeds with the infiltration of the bone-lining cell layer to reach the bone surface and resorb bone minerals.<sup>3</sup> However, the mechanism behind the migration of these osteoclast precursors toward resorption sites remains unclear.

Previous studies have demonstrated that extracellular calcium ions ( $\text{Ca}^{2+}$ ),<sup>5</sup> and some chemokines, e.g., CX3CL1<sup>21</sup> or blood-enriched lipid mediator sphingosine-1-phosphate (S1P),<sup>16</sup> regulate the localization and homing of osteoclasts or their precursors.<sup>16,21</sup> However, the functions of mechanical cues in this process are seldom considered. The bone matrix becomes deformed when bone tissue is mechanically loaded, and the deformation drives the interstitial fluid within the cavities to flow over the surfaces of the trabeculae or lacunae, causing the osteoclasts or osteoblasts on the surfaces to suffer from fluid shear stress (FSS).<sup>32</sup> Some *in vivo*<sup>11,17</sup> and *in vitro*<sup>25</sup> studies have shown that FSS can activate the differentiation of osteoclasts and further regulate bone resorption. Our previous study has found that FSS can induce calcium response in both osteoclasts and their precursors.<sup>23,24</sup> Other mechanical stimulations, such as the single-cell indentation by a glass pipette<sup>40–42</sup> or whole-cell membrane stretching by changing osmotic pressure,<sup>33</sup> can also result in a significant intracellular calcium response in osteoclasts. However, whether mechanical loading involves in the migration of osteoclasts and what the molecular mechanism is remains unknown.

---

Address correspondence to Bo Huo and Baohua Ji, Biomechanics and Biomaterials Laboratory, Department of Mechanics, School of Aerospace Engineering, Beijing Institute of Technology, No. 5 South Zhongguancun Street, Beijing 100081, People's Republic of China. Electronic mails: huobo@bit.edu.cn and bhji@bit.edu.cn

Calcium ions are among the most important secondary messengers in cells. Previous studies have shown that intracellular calcium dynamics is closely related to cell migration behaviors, such as an increase in calcium concentration from the front to the rear of migrating cells at a relatively long time-scale<sup>7,28,37</sup> and a calcium flicker with front-to-rear polarization at a short timescale.<sup>37</sup> Our recent study has shown that the mechanosensitive, cation-selective channels (MSCC), phospholipase C (PLC), and endoplasmic reticulum (ER) are the major signaling pathways for mechanical stimulation-induced calcium response in RAW264.7 osteoclastic precursors (monocytes).<sup>24</sup> In this study, we test the hypothesis that calcium signaling pathways may be involved in FSS-induced cell migration.

RAW264.7 monocytes were exposed to 1 and 10 dyne/cm<sup>2</sup> FSS for 30 min, after which the dynamic parameters of cell migration were analyzed. The results showed that the RAW264.7 cells tended to migrate along the flow direction and that the migration speed and orientation increased with FSS level. Three calcium pathways (i.e., MSCC, ER, or extracellular calcium) had significant impact on their migration. When one of the three is blocked, the migration speed along flow direction is significantly reduced. The osteoclasts induced for 4 or 8 days also preferentially migrated along the direction of fluid flow, but calcium pathways did not influence their migration.

## MATERIALS AND METHODS

### Cell Culture

The osteoblast-like MC3T3-E1 cell line was purchased from the American Type Culture Collection (ATCC, Manassas, USA) and cultured in alpha modified eagle's medium ( $\alpha$ -MEM, Hyclone, USA) supplemented with 10% fetal bovine serum (FBS, Gibco, USA), 100 units/mL of penicillin (Sigma, St. Louis, USA), and 100 units/mL streptomycin (Sigma, St. Louis, USA). The medium was changed every 48 h, and the conditioned medium was collected every 24 h when cells reached 70% confluence. The RAW264.7 cell line was purchased from the European Collection of Cell Cultures (ECACC, Wiltshire, UK) and cultured in Dulbecco's modified eagle's medium (DMEM, Hyclone, USA) supplemented with 10% FBS, 100 units/mL of penicillin, and 100 units/mL of streptomycin. As described in our previous study,<sup>23</sup> the mononuclear RAW264.7 cells were induced to fuse or differentiate into TRAP-positive multinucleated osteoclasts with a 1:1 mixture of the DMEM medium and the conditioned medium from MC3T3-E1 cells.

### FSS Stimulation and Calcium Signaling Pathways

The RAW264.7 monocytes or the induced osteoclasts were seeded on plastic slides (NUNC, Roskilde, Denmark) at a density of  $2 \times 10^4$ /cm<sup>2</sup>. The slides were mounted on the custom-made parallel flow chamber after 24 h of cell seeding (Fig. 1c). An FSS level of 1 or 10 dyne/cm<sup>2</sup> was adopted to stimulate the cells for 30 min, during which time-lapse images were recorded at 30 s intervals by using a Leica DMI 6000B inverted microscope (Fig. 1a). These images were used to analyze cell migration parameters. Similar to our previous study,<sup>24</sup> five pathways of calcium signaling were investigated by incubating the slides with blocking reagents before cells are exposed to FSS. In brief, 10  $\mu$ M Gadolinium chloride (Gd<sup>3+</sup>, Sigma, St. Louis, USA) was supplied as the MSCC blocker, the calcium stored in the ER was depleted with 1  $\mu$ M thapsigargin (TG, Sigma, St. Louis, USA), and 10  $\mu$ M U73122 (Calbiochem, Darmstadt, Germany) was adopted to inhibit PLC. For the above blocking tests, 10 min incubation of chemical reagents was applied. Extracellular calcium was removed by using calcium-free DMEM (Gibco, Carlsbad, USA). 100  $\mu$ M suramin was used to block adenosine triphosphate (ATP) binding with P2 purinergic receptors during the 30 min incubation. It should be noted that the blocking reagents were maintained during FSS stimulation.

### Cell Migration Assay

The geometric parameters of migrating cells were quantified by a program developed with Matlab software. Cells that are already or going to be in contact with other cells were excluded. Edge extraction and dilation were used to obtain the general outline of a cell; the internal holes were filled, and the cell was treated with an erosion process to remove the small regions (Fig. 1b). The centroid of a cell was adopted as its position, around which a rectangular region twice the cell size was defined to calculate the position of the migrating cell in the next image through digital image correlation (DIC).<sup>6</sup> The cell trajectory path was determined after its position has been identified. The location shift was calibrated by using a fixed point in the field.

Cell migration is mainly analyzed by using the parameters shown in Fig. 1d. The total distance that the cell traveled in time  $t$  is calculated by  $S_g = \sum_{i=1}^n S_i$ , where  $S_i$  is the distance traveled by the cell in 1.5 min. Therefore, the general speed is  $S_g/t$ . The relative displacement  $S_l$  is shown by the red arrow between the start and end points of the cellular trajectory in Fig. 1d. The inclined angle  $\theta_p$  between the cell trajectory and the flow direc-

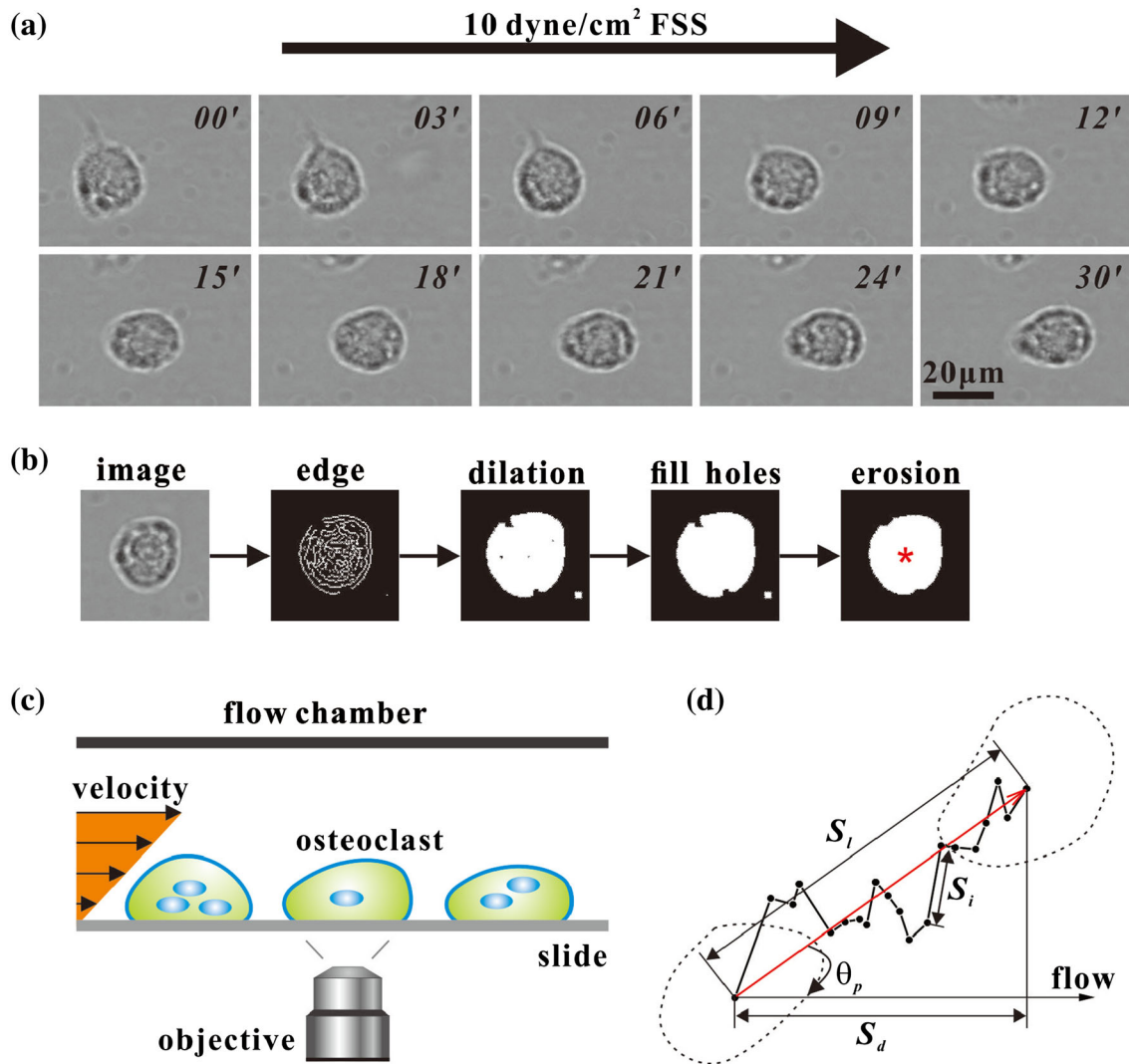


**FIGURE 1.** Migration of RAW264.7 cells under shear flow. (a) Time-lapsed images of an individual RAW264.7 cell exposed to 10 dyne/cm<sup>2</sup> FSS; the arrow shows the flow direction. (b) Image processing of a migrating cell; the red star indicates the centroid of this cell adopted as its position. (c) Sketch map of a parallel-plate flow chamber system. (d) Definition of the migration parameters.  $S_i$  is the distance of cell movement in a given time interval,  $n$  is the number of time intervals, the general distance of cell migration is denoted as  $S_g = \sum_{i=1}^n S_i$ . The red arrow is the direct line connecting the initial and end positions of a migration cell and  $S_i$  and  $\theta_p$  are the line's length and angle relative to the flow direction, respectively.

tion represent migration orientation. Cell speed along the flow direction is  $S_d/t = S_i \times \cos \theta_p/t$ , which indicates the capability of the cell to adapt to the fluid flow. The directionality  $S_i/S_g$  shows the tendency of a cell to move along a direct line. A directionally migrating cell registers migration speed and directionality that are larger than the mean value plus standard deviation (SD), which indicates that no flow is applied.

#### Statistical Analysis

More than three slides (at least 60 cells) were tested for a specific induction time, FSS level, and chemical

blocking. All the results were expressed as mean  $\pm$  SD. Statistical differences between the mean values of different groups were determined by using one-way ANOVA, and were considered significant when  $p < 0.05$  if not specifically claimed.

## RESULTS

### FSS Stimulates RAW264.7 Cells to Migrate

The time-lapsed images of RAW264.7 cells recorded for 30 min with or without 1 and 10 dyne/cm<sup>2</sup> FSS showed that the effect of FSS on cell migration is dose-dependent (Fig. 2). When no flow was applied, cells

migrated randomly. For 1 dyne/cm<sup>2</sup> FSS, most cells migrated along the flow direction, and the inclined angle  $\theta_p$  between the cell migration and fluid flow directions are uniformly distributed within the range  $-90^\circ$  to  $90^\circ$  (Fig. 2a). The average value of  $\cos \theta_p$  was 0.47, which was significantly higher than that in the no-flow group (Fig. 2b). For the 10 dyne/cm<sup>2</sup> FSS group, almost all cells migrated within a narrow  $\pm 30^\circ$  range of  $\theta_p$ ; more than 40% of these cells were within the  $\pm 15^\circ$  range (Fig. 2a). In addition, the value of  $\cos \theta_p$  (0.70) was significantly larger than that (0.47) under 1 dyne/cm<sup>2</sup> FSS (Fig. 2b). When excluding the randomly migrating cells,  $\cos \theta_p$  was 0.77 for 10 dyne/cm<sup>2</sup> FSS group (Fig. 2c).

The directionalities for 1 and 10 dyne/cm<sup>2</sup> FSS were 0.26 and 0.37, respectively, both of which were significantly higher than that in the no-flow group (Fig. 2d). This observation implies that increased FSS levels promote the cells to migrate along a straight line rather than a curved trajectory. Meanwhile, 25 or 65% of directionally migrating cells for 1 or 10 dyne/cm<sup>2</sup> FSS, respectively, were also significantly more than that in the static group (10%) (Fig. 2e). The migration speed of the no-flow group was nearly zero, but the speed along the flow was increased to 0.09 and 0.29  $\mu\text{m}/\text{min}$  for 1 and 10 dyne/cm<sup>2</sup> FSS, respectively (Fig. 2f). Figure 2g shows that the general migration speed has no obvious correlation with directionality.

#### *Calcium Signaling Pathways Involved in the FSS-Induced Migration of RAW264.7 Cells*

Five pathways, i.e., MSCC, PLC, ATP, ER, and extracellular calcium, were chemically blocked by  $\text{Gd}^{3+}$ , U73122, suramin, TG, and  $\text{Ca}^{2+}$ -free medium, respectively, to test whether intracellular calcium signaling pathways are involved in the FSS-induced migration of RAW264.7 monocytes. The properties of cell migration were also analyzed. For the control group with 10 dyne/cm<sup>2</sup> FSS, 44% of the cells migrated within  $\pm 15^\circ$  relative to the flow direction, whereas 12.5% of the cells migrated against the flow (Fig. 3a). However, for the  $\text{Gd}^{3+}$ , TG, U73122, and  $\text{Ca}^{2+}$ -free groups, the cells that migrated within  $\pm 15^\circ$  significantly decreased to 28.3, 25.2, 24.7, and 33.3%, respectively, and those that migrated against flow increased to 24.5, 18.7, 17.8, and 28.4%, respectively. Inhibiting the ATP pathway did not affect cell migration.

Figure 3b shows that when the MSCC, ER and extracellular calcium pathways were inhibited, the cell speed along flow direction was significantly reduced to 0.17, 0.18, and 0.17  $\mu\text{m}/\text{min}$ , respectively, compared with 0.29  $\mu\text{m}/\text{min}$  for the control group. Blocking the PLC or ATP pathway did not affect the speed. Inter-

estingly, the general speed along the trajectory was not significantly reduced when blocking either of these pathways (Fig. 3c). The direction of cell migration along the flow, such as  $\cos \theta_p$ , was only reduced by blocking MSCC pathway (Fig. 3d). Furthermore, the directionalities of  $\text{Gd}^{3+}$  and  $\text{Ca}^{2+}$ -free groups significantly decreased to 0.27 and 0.28, respectively, compared with 0.37 for the control group (Fig. 3e).

#### *Differentiated Osteoclasts Migrate Under FSS But Cannot be Regulated by Calcium Signaling Pathways*

After the RAW264.7 cells were induced to differentiate into osteoclasts, no significant difference was observed (Fig. 4a). The speed of FSS-induced migration in the FSS direction were 0.29, 0.31, and 0.36  $\mu\text{m}/\text{min}$  for 0, 4, and 8 days induction, respectively. Similarly, the general speed and migration orientation ( $\cos \theta_p$ ) of cells was also independent of induction time (Figs. 4b and 4c). Additionally, the differentiated osteoclasts after 8 d induction exhibited higher directionality (0.46) than RAW264.7 monocytes (0.37) but no significant difference was found (Fig. 4d). Figure 5 shows the effect of calcium signaling pathways on FSS-induced migration of osteoclasts. No significant difference was detected for different calcium pathways for RAW264.7 cells induced for 4 or 8 days.

## DISCUSSION

The present study demonstrated that FSS promoted the migration of RAW264.7 monocytes as well as differentiated osteoclasts induced by the conditioned medium from osteoblasts (Figs. 2 and 4). Except for a few randomly migrating cells, most of the cells migrated along the flow direction. The migration of pre-osteoclasts and mature osteoclasts in FSS was dose-dependent, i.e., the speed along the flow direction, inclined angle, and directionality were remarkably enhanced when FSS level was increased from 1 to 10 dyne/cm<sup>2</sup>. The general migration speed without fluid flow is 0.49  $\mu\text{m}/\text{min}$ , close to the recent result indicating that the out growth rate of osteoclast lamellipod is 0.7  $\mu\text{m}/\text{min}$ .<sup>39</sup> Similarly, an *in vivo* study on the migration of osteoclast precursor monocytes showed that cells treated with vehicle, active vitamin D metabolite (1,25-D) and eldcalcitol (ELD), respectively, had migration speeds of 1.9, 2.4, and 2.4  $\mu\text{m}/\text{min}$ .<sup>19</sup> The flow-induced migration has been observed in other cell types, e.g., FSS by blood flow increased the migration speed of vascular endothelial cells.<sup>9,30</sup> However, the FSS does not always monotonically enhance cell migration along flow direction. For

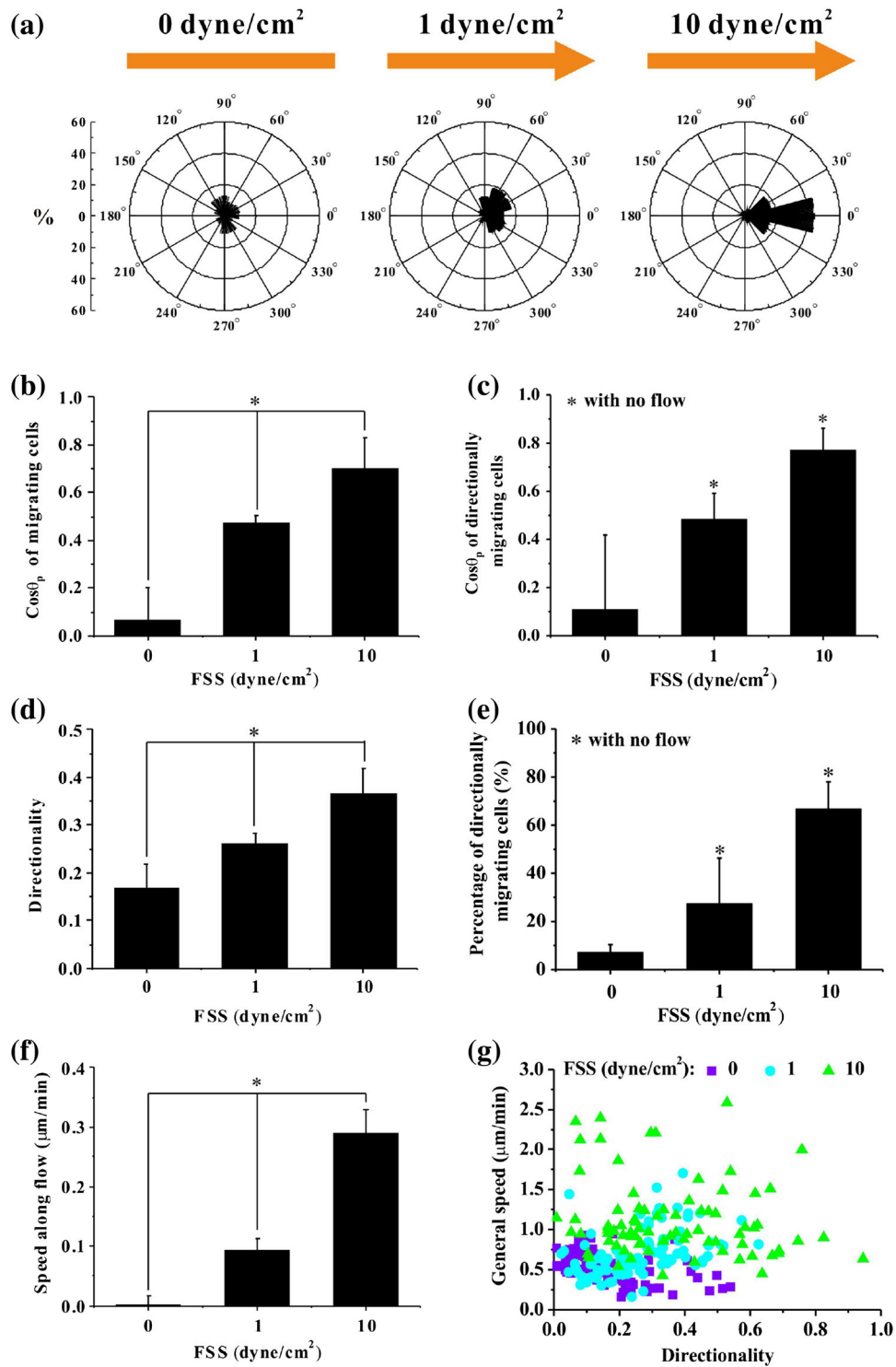
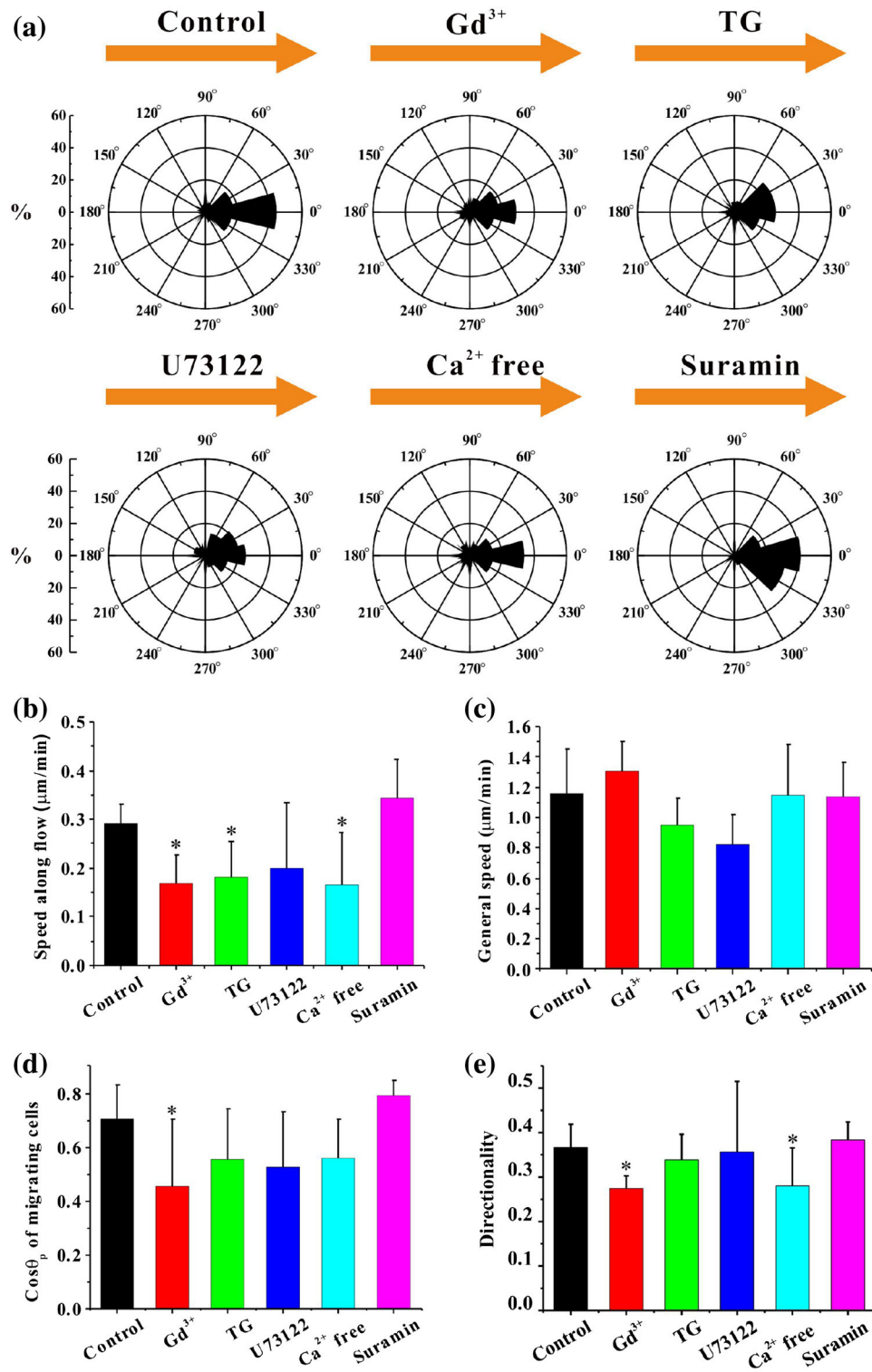
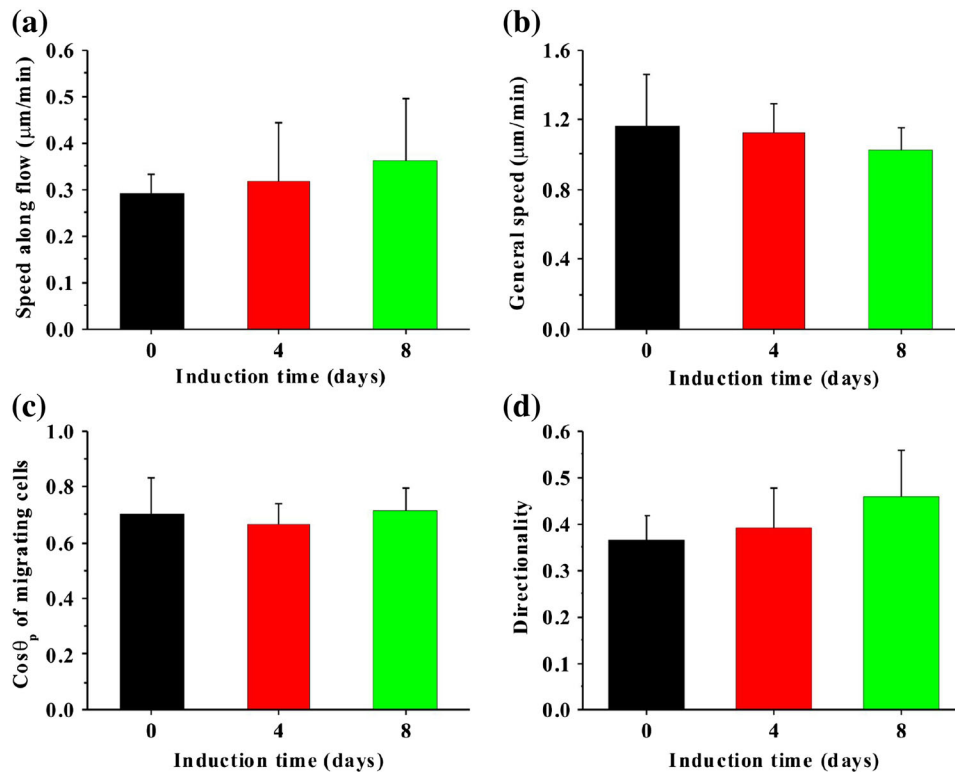


FIGURE 2. Regulation of FSS levels on RAW264.7 cell migration. (a) Rose diagrams of cell migration at static state or when exposed to 1 and 10 dyne/cm<sup>2</sup> FSS; the area of a sector with 30° central angle indicates the percentage of cells migrating along the corresponding orientation  $\theta_p$ . (b) and (c),  $\cos \theta_p$  of migrating and directionally migrating cells. (d) Directionality of migrating cells. (e) Percentage of directionally migrating cells. (f) The speed of cell migration along flow direction. (g) The general speed of migrating cells vs. the directionality. Data are shown as mean  $\pm$  SD. Each group has at least 60 cells from three independent experiments \* $p < 0.05$ .



**FIGURE 3.** Effect of calcium signaling pathways on FSS-induced RAW264.7 cell migration. (a) Rose diagrams of cell migration treated with different calcium signaling inhibitors; the area of a sector with 30° central angle indicates the percentage of cells migrating along the corresponding orientation  $\theta_p$ . (b)–(e) Speed along flow direction, general speed,  $\text{cos}\theta_p$  and directionality of migrating cells. The cells are exposed to 10 dyne/cm<sup>2</sup> FSS. Data are shown as mean  $\pm$  SD. Each group has at least 60 cells from three independent experiments \* $p < 0.05$ .



**FIGURE 4.** Effect of induction time (0, 4, or 8 days) on FSS-induced migration parameters, speed along flow direction (a), general speed (b),  $\cos \theta_p$  (c) and directionality (d). The cells are exposed to  $10 \text{ dyne/cm}^2$  FSS. Data are shown as mean  $\pm$  SD. Each group has at least 60 cells from three independent experiments.

example, when endothelial and smooth muscle cells were co-cultured, FSS delayed the onset of dose-dependent migration.<sup>20</sup> In addition, although FSS of  $2\text{--}10 \text{ dyne/cm}^2$  can induce the migration of human mesenchymal stem cells (hMSCs) with notably higher speed than the statically cultured hMSCs, FSS larger than  $20 \text{ dyne/cm}^2$  markedly inhibited migration.<sup>35</sup> Interestingly, the breast cancer cells seeded at high density in 3D gel expectedly migrated against, rather than with, the flow.<sup>27</sup> To clarify the relations between cell migration, cell type and mechanical loading may require more extensive and quantitative experiments as well as theoretical analysis basing on the dynamics of cell adhesion.<sup>14,22,43</sup>

The migration of osteoclast starts from the mononucleated precursors in the capillaries of bone microcirculation system and ends at the periosteum close to bone surfaces that encompass the trabecular and intramedullary cavities. The wall shear stress of blood flow in postcapillary venule is approximately  $3 \text{ dyne/cm}^2$ .<sup>29</sup> Therefore the physiological FSS level for pre-osteoblasts should be around  $3 \text{ dyne/cm}^2$ . When osteoclasts arrive at bone surface, they will experience the shear stress from interstitial fluid flow, similar to osteoblasts. For osteocytes located within lacunae, some theoretical analysis suggested that FSS was on

the order of  $8\text{--}30 \text{ dyne/cm}^2$ .<sup>38</sup> Since the size of trabecular cavities is much larger than that of lacunae-canalculi system, the FSS level for osteoclasts should be lower than that for osteocytes. In fact, the flow rate or FSS at bone surface still remains unknown due to the difficulty of *in vivo* experimental observation. In this study, we adopted  $1$  or  $10 \text{ dyne/cm}^2$  FSS, which is in the range between the FSS in postcapillary venule and that in lacunae.

Bone resorption and subsequent bone formation usually occur around a microdamage to secure skeletal integrity, which is called targeted remodeling.<sup>10</sup> But it is still unclear how the mononuclear pre-osteoclasts in the periosteum migrate to the resorption sites on bone surface.<sup>2,3</sup> Many researchers believed that the apoptotic osteocytes near the microdamage released cytokines such as RANKL, phosphatidylserine, ICAM-3 or CD31 to regulate the recruitment and differentiation of osteoclasts.<sup>1,8,18</sup> But the roles of mechanical cues on the bone resorption is seldom studied. In fact, one study has demonstrated that osteocyte apoptosis may be insufficient for repairing microdamage without mechanical stimulation.<sup>34</sup> When the bone is loaded or unloaded, the interstitial fluid permeates the lacunar-canalicular, trabecular, or medullary cavities.<sup>12</sup> According to fluid mechanics and the findings of this article, fluid velocity

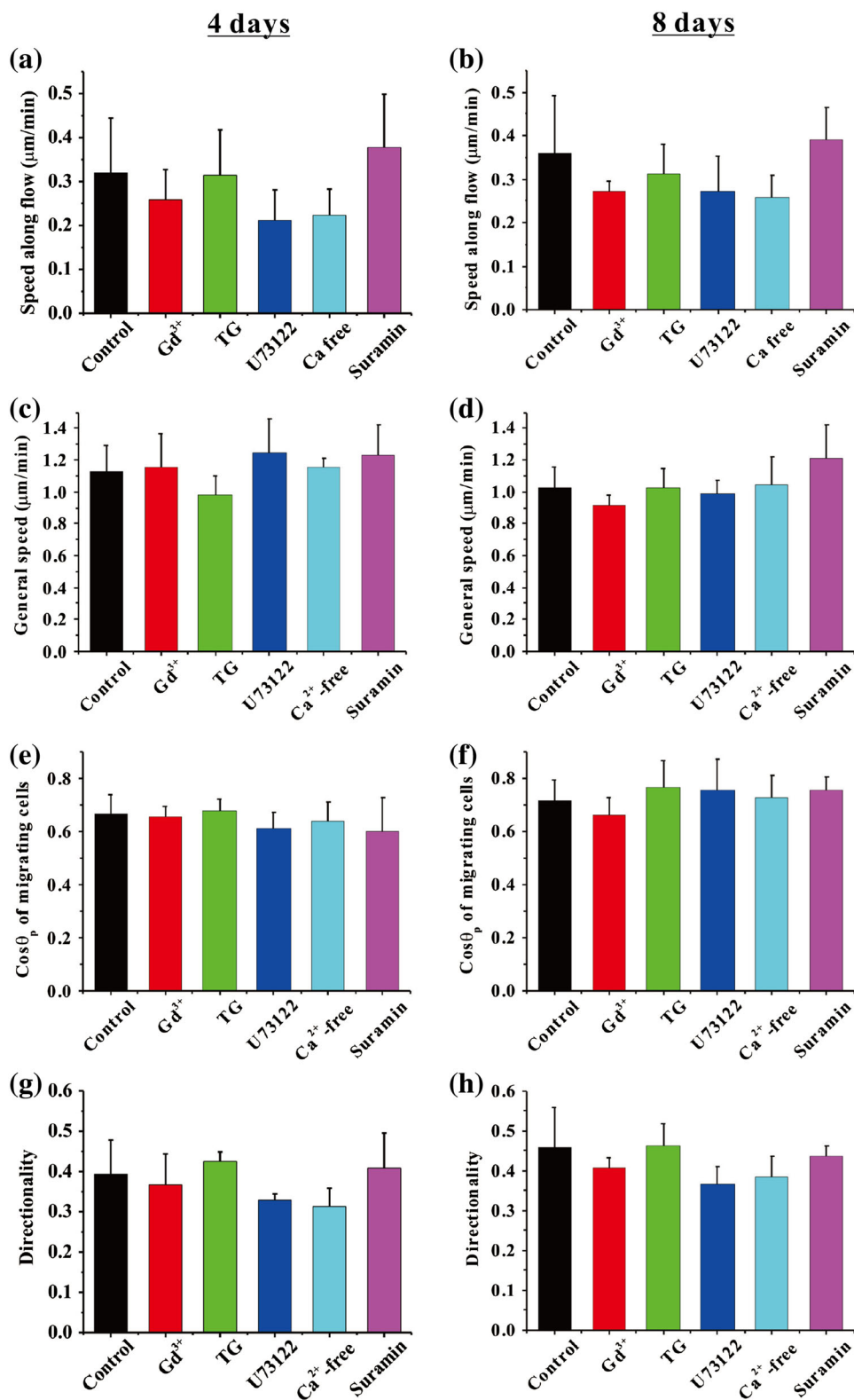
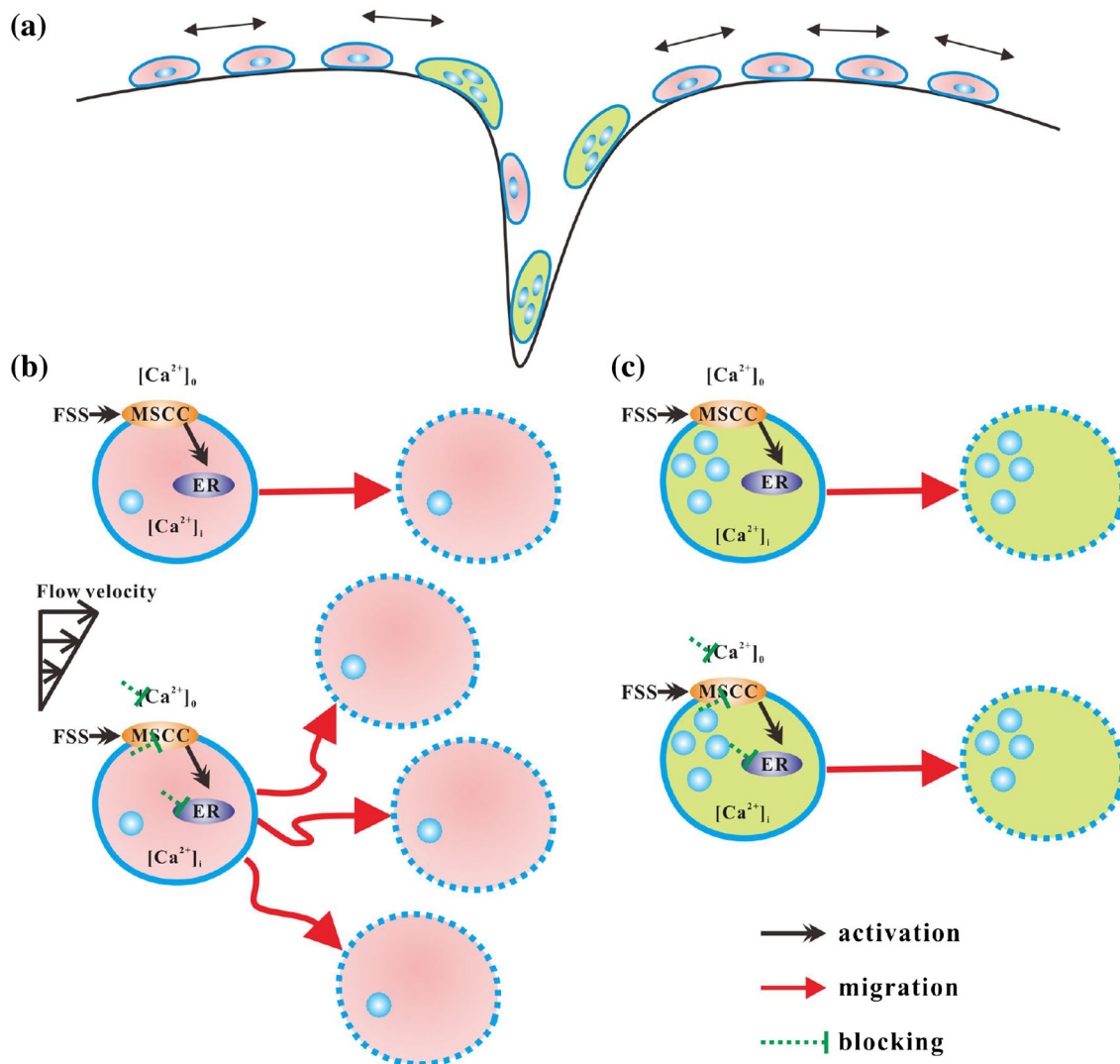


FIGURE 5. Calcium signaling pathways not involved in FSS-induced migration of differentiated osteoclasts. The RAW264.7 monocytes were induced for 4 or 8 d and the osteoclasts are exposed to 10 dyne/cm<sup>2</sup> FSS. Data are shown as mean  $\pm$  SD. Each group has at least 60 cells from three independent experiments.





**FIGURE 6.** Schematics of FSS-induced migration of monocytes and multinucleated osteoclasts as well as the signaling pathways. (a) Cells migrate on bone surface driven by fluid flow but pool inside a microdamage, in which double-headed arrows indicate the oscillating flow. (b) For the mononuclear preosteoclasts, FSS activates the calcium signaling pathways to regulate the cell migration along flow direction. When the pathway is inhibited, the cells lose the ability to sense the flow direction and will migrate randomly. (c) When the monocytes fuse into multinucleated osteoclasts, calcium signaling pathways will not combine with the flow-induced FSS migration although FSS can still stimulate their migration.

may decrease quickly from bone surface to the inside of a microdamage so that the pre-osteoclastic monocytes or osteoclasts may sink or pool in it (Fig. 6a). There are usually two kinds of fatigue-induced microdamages, i.e., large crack with 10–100  $\mu\text{m}$  in length, which is comparable with the size of osteoclasts,<sup>23</sup> and diffuse damage with submicron size. The previous studies have found that bone resorption occurred at larger crack but not in diffuse damage.<sup>4,15,36</sup> For the diffuse damage, osteoclasts or monocytes may be driven away by fluid flow so as to inhibit the bone resorption over there. Therefore our present result can provide an alternative explanation for targeted bone remodeling.

The present study also showed that calcium signaling pathways, such as MSCC, ER and extracellular calcium, involved in the FSS induced-migration of RAW264.7 cells (Fig. 3). It should be noted that the primary pathways are similar to those in our previous study on FSS-induced  $[Ca^{2+}]_i$  response except PLC.<sup>23</sup> Our current results indicated that when any of these pathways was blocked, the speed along the flow direction was significantly reduced, and the general speed did not change significantly (Fig. 3c), which suggest that fluid flow-induced intracellular calcium response only regulates the migration direction of pre-osteoclasts rather than their migration capability.

Previous studies have shown that the blockade of  $[Ca^{2+}]_0$  influx into the body of kidney cells slows down the migration to 47% in the control.<sup>28</sup> The excellent discovery of calcium flicker in migrating fibroblasts provides more evidence of the functions of MSCC,  $[Ca^{2+}]_0$ , and  $[Ca^{2+}]_i$ ,<sup>37</sup> in which calcium flicker activity was dually coupled to TRPM7, a stretch activated transient receptor potential ion channel, as well as inositol-1,4,5-trisphosphate receptors on internal calcium stores. A recent study with the isolated osteoclasts showed that the lamellipodia outgrowth occurs steadily at a rate of  $\sim 0.7 \mu\text{m}/\text{min}$ .<sup>39</sup> The intracellular calcium elevation at the uropod during migration initiated uropod retraction, whereas the dissipation of this  $[Ca^{2+}]_i$  gradient by loading osteoclasts with the  $Ca^{2+}$  chelator BAPTA abolished uropod retraction. Therefore, it is reasonable to deduce that fluid flow may induce the gradient distribution of  $[Ca^{2+}]_i$  within an osteoclast, after which the local calcium gradient regulates the dynamics of focal adhesion at the front or rear parts and further controls the directional migration. More investigations need to be done to clarify the relation between intracellular calcium gradient and osteoclast migration.

For RAW264.7 cells induced for 4 or 8 d, the present results (Fig. 5) showed that the calcium signaling pathways were not involved in osteoclast migration, which is significantly different from their undifferentiated states. Our previous study has shown that under FSS stimulations, small osteoclasts possess more calcium responsive peaks than large osteoclasts.<sup>23</sup> Increasing FSS enhances the calcium oscillation of osteoclasts at early induction but impedes it at late induction. Furthermore, the calcium responsive sensitivity of osteoclasts to FSS is reduced along with the fusion of osteoclasts. Similarly, another study on RANKL-induced calcium oscillation for osteoclasts with different nuclei has indicated that the capability for calcium oscillation in the early differentiation is stronger than that in late differentiation.<sup>26</sup> These results imply that the cells become tardy in the calcium response to fluid flow stimulation at the terminal differentiation stage of osteoclasts, thereby resulting in the halting of motile osteoclasts so that they serve their function of resorbing bone minerals.

In conclusion, this study shows that fluid flow first activates the calcium signaling pathways and then regulates the cellular migration along flow direction in mononuclear osteoclasts (Fig. 6). If the pathways are inhibited, the cells lose the capability to sense the flow direction and will migrate randomly. When the monocytes fuse into multinucleated osteoclasts, calcium signaling pathways will not be involved in flow-induced migration.

## ACKNOWLEDGMENTS

This work was supported by the National Natural Science Foundation of China [11372043 (BH), 11025208, 11372042, and 11221202 (BJ)] and the Fundamental Research Funds for the Central Universities [GZ2013015101 (BH)].

## CONFLICT OF INTEREST

Chenglin Liu, Shuna Li, Baohua Ji, and Bo Huo declare that they have no conflicts of interest.

## ETHICAL STANDARDS

No human or animal studies were carried out by the authors for this article.

## REFERENCES

- <sup>1</sup>Al-Dujaili, S. A., E. Lau, *et al.* Apoptotic osteocytes regulate osteoclast precursor recruitment and differentiation *in vitro*. *J. Cell Biochem.* 112(9):2412–2423, 2011.
- <sup>2</sup>Baron, R., L. Neff, *et al.* Kinetic and cytochemical identification of osteoclast precursors and their differentiation into multinucleated osteoclasts. *Am. J. Pathol.* 122(2):363–378, 1986.
- <sup>3</sup>Baroukh, B., M. Cherruau, *et al.* Osteoclasts differentiate from resident precursors in an *in vivo* model of synchronized resorption: a temporal and spatial study in rats. *Bone* 27(5):627–634, 2000.
- <sup>4</sup>Bentolila, V., T. M. Boyce, *et al.* Intracortical remodeling in adult rat long bones after fatigue loading. *Bone* 23(3):275–281, 1998.
- <sup>5</sup>Boudot, C., Z. Saidak, *et al.* Implication of the calcium sensing receptor and the phosphoinositide 3-kinase/Akt pathway in the extracellular calcium-mediated migration of RAW 264.7 osteoclast precursor cells. *Bone* 46(5):1416–1423, 2010.
- <sup>6</sup>Bruck, H. A., S. R. McNeill, *et al.* Digital image correlation using Newton–Raphson method of partial-differential correction. *Exp. Mech.* 29(3):261–267, 1989.
- <sup>7</sup>Brundage, R. A., K. E. Fogarty, *et al.* Calcium gradients underlying polarization and chemotaxis of eosinophils. *Science* 254(5032):703–706, 1991.
- <sup>8</sup>Cardoso, L., B. C. Herman, *et al.* Osteocyte apoptosis controls activation of intracortical resorption in response to bone fatigue. *J. Bone Miner. Res.* 24:597–605, 2008.
- <sup>9</sup>Chandran, P., A. Sasidharan, *et al.* Highly biocompatible TiO(2):Gd(3)(+) nano-contrast agent with enhanced longitudinal relaxivity for targeted cancer imaging. *Nanoscale* 3(10):4150–4161, 2011.
- <sup>10</sup>Eriksen, E. F. Cellular mechanisms of bone remodeling. *Rev. Endocr. Metab. Disord.* 11(4):219–227, 2010.
- <sup>11</sup>Fahlgren, A., M. P. G. Bostrom, *et al.* Fluid pressure and flow as a cause of bone resorption. *Acta Orthop.* 81(4):508–516, 2010.
- <sup>12</sup>Gardinier, J. D., C. W. Townend, *et al.* *In situ* permeability measurement of the mammalian lacunar-canalicular system. *Bone* 46(4):1075–1081, 2010.

- <sup>13</sup>Hadjidakis, D. J., and I. I. Androulakis. Bone remodeling. *Ann. NY Acad. Sci.* 1092:385–396, 2006.
- <sup>14</sup>He, S., Y. Su, *et al.* Some basic questions on mechanosensing in cell-substrate interaction. *J. Mech. Phys. Solids* 70:116–135, 2014.
- <sup>15</sup>Herman, B. C., L. Cardoso, *et al.* Activation of bone remodeling after fatigue: differential response to linear microcracks and diffuse damage. *Bone* 47(4):766–772, 2010.
- <sup>16</sup>Ishii, M., J. Kikuta, *et al.* Chemorepulsion by blood S1P regulates osteoclast precursor mobilization and bone remodeling *in vivo*. *J. Exp. Med.* 207(13):2793–2798, 2010.
- <sup>17</sup>Johansson, L., U. Edlund, *et al.* Bone resorption induced by fluid flow. *J. Biomech. Eng.* 131(9):094505, 2009.
- <sup>18</sup>Kennedy, O. D., B. C. Herman, *et al.* Activation of resorption in fatigue-loaded bone involves both apoptosis and active pro-osteoclastogenic signaling by distinct osteocyte populations. *Bone* 50(5):1115–1122, 2012.
- <sup>19</sup>Kikuta, J., S. Kawamura, *et al.* Sphingosine-1-phosphate-mediated osteoclast precursor monocyte migration is a critical point of control in antibone-resorptive action of active vitamin D. *Proc. Natl. Acad. Sci. USA* 110(17):7009–7013, 2013.
- <sup>20</sup>Kim, S. Y., S. H. Park, *et al.* Mechanical stimulation and the presence of neighboring cells greatly affect migration of human mesenchymal stem cells. *Biotechnol. Lett.* 35(11):1817–1822, 2013.
- <sup>21</sup>Koizumi, K., Y. Saitoh, *et al.* Role of CX3CL1/fractalkine in osteoclast differentiation and bone resorption. *J. Immunol.* 183(12):7825–7831, 2009.
- <sup>22</sup>Kong, D., B. H. Ji, *et al.* Stabilizing to disruptive transition of focal adhesion response to mechanical forces. *J. Biomech.* 43(13):2524–2529, 2010.
- <sup>23</sup>Li, P., M. Hu, *et al.* Fluid flow-induced calcium response in early or late differentiated osteoclasts. *Ann. Biomed. Eng.* 40(9):1874–1883, 2012.
- <sup>24</sup>Li, P., C. Liu, *et al.* Fluid flow-induced calcium response in osteoclasts: signaling pathways. *Ann. Biomed. Eng.* 42(6):1250–1260, 2014.
- <sup>25</sup>Liu, Y., L. Li, *et al.* Effects of fluid shear stress on bone resorption in rat osteoclasts. *J. Biomech. Eng.* 24(3):544–548, 2007.
- <sup>26</sup>Masuyama, R., J. Vriens, *et al.* TRPV4-mediated calcium influx regulates terminal differentiation of osteoclasts. *Cell Metab.* 8(3):257–265, 2008.
- <sup>27</sup>Polacheck, W. J., J. L. Charest, *et al.* Interstitial flow influences direction of tumor cell migration through competing mechanisms. *Proc. Natl. Acad. Sci. USA* 108(27):11115–11120, 2011.
- <sup>28</sup>Schwab, A., F. Finsterwalder, *et al.* Intracellular Ca<sup>2+</sup> distribution in migrating transformed epithelial cells. *Pflügers Arch.* 434(1):70–76, 1997.
- <sup>29</sup>Sheikh, S., G. E. Rainger, *et al.* Exposure to fluid shear stress modulates the ability of endothelial cells to recruit neutrophils in response to tumor necrosis factor- $\alpha$ : a basis for local variations in vascular sensitivity to inflammation. *Blood* 102(8):2828–2834, 2003.
- <sup>30</sup>Shiu, Y. T., S. Li, *et al.* Rho mediates the shear-enhancement of endothelial cell migration and traction force generation. *Biophys. J.* 86(4):2558–2565, 2004.
- <sup>31</sup>Teitelbaum, S. L. Bone resorption by osteoclasts. *Science* 289(5484):1504–1508, 2000.
- <sup>32</sup>Thompson, W. R., C. T. Rubin, *et al.* Mechanical regulation of signaling pathways in bone. *Gene* 503(2):179–193, 2012.
- <sup>33</sup>Tsuzuki, T., K. Okabe, *et al.* Osmotic membrane stretch increases cytosolic Ca(2+) and inhibits bone resorption activity in rat osteoclasts. *Jpn. J. Physiol.* 50(1):67–76, 2000.
- <sup>34</sup>Waldorff, E. I., K. B. Christenson, *et al.* Microdamage repair and remodeling requires mechanical loading. *J. Bone Miner. Res.* 25(4):734–745, 2010.
- <sup>35</sup>Wang, H., W. Sun, *et al.* Polycystin-1 mediates mechanical strain-induced osteoblastic mechanoresponses via potentiation of intracellular calcium and Akt/beta-catenin pathway. *PLoS One* 9(3):e91730, 2014.
- <sup>36</sup>Wang, L., T. Ye, *et al.* Repair of microdamage in osteonal cortical bone adjacent to bone screw. *PLoS One* 9(2):e89343, 2014.
- <sup>37</sup>Wei, C., X. Wang, *et al.* Calcium flickers steer cell migration. *Nature* 457(7231):901–905, 2009.
- <sup>38</sup>Weinbaum, S., S. C. Cowin, *et al.* A model for the excitation of osteocytes by mechanical loading-induced bone fluid shear stresses. *J. Biomech.* 27(3):339–360, 1994.
- <sup>39</sup>Wheal, B. D., R. J. Beach, *et al.* Subcellular elevation of cytosolic free calcium is required for osteoclast migration. *J. Bone Miner. Res.* 29(3):725–734, 2014.
- <sup>40</sup>Wiebe, S. H., S. M. Sims, *et al.* Calcium signalling via multiple P2 purinoceptor subtypes in rat osteoclasts. *Cell. Physiol. Biochem.* 9(6):323–337, 1999.
- <sup>41</sup>Xia, S. L., and J. Ferrier. Calcium signal induced by mechanical perturbation of osteoclasts. *J. Cell. Physiol.* 163(3):493–501, 1995.
- <sup>42</sup>Xia, S. L., and J. Ferrier. Localized calcium signaling in multinucleated osteoclasts. *J. Cell. Physiol.* 167(1):148–155, 1996.
- <sup>43</sup>Zhong, Y., and B. Ji. How do cells produce and regulate the driving force in the process of migration? *Eur. Phys. J. Spec. Top.* 223(7):1373–1390, 2014.